

# Fractional Brownian motion and the critical dynamics of zipping polymers

J.-C. Walter, A. Ferrantini, and E. Carlon

*Institute for Theoretical Physics, KULeuven, Celestijnenlaan 200D, B-3001 Leuven, Belgium*

C. Vanderzande

*Faculty of Sciences, Hasselt University, Agoralaan 1, B-3590 Diepenbeek, Belgium and  
Institute for Theoretical Physics, KULeuven, Celestijnenlaan 200D, B-3001 Leuven, Belgium*

(Dated: November 6, 2018)

We consider two complementary polymer strands of length  $L$  attached by a common end monomer. The two strands bind through complementary monomers and at low temperatures form a double stranded conformation (zipping), while at high temperature they dissociate (unzipping). This is a simple model of DNA (or RNA) hairpin formation. Here we investigate the dynamics of the strands at the equilibrium critical temperature  $T = T_c$  using Monte Carlo Rouse dynamics. We find that the dynamics is anomalous, with a characteristic time scaling as  $\tau \sim L^{2.26(2)}$ , exceeding the Rouse time  $\sim L^{2.18}$ . We investigate the probability distribution function, the velocity autocorrelation function, the survival probability and boundary behavior of the underlying stochastic process. These quantities scale as expected from a fractional Brownian motion with a Hurst exponent  $H = 0.44(1)$ . We discuss similarities and differences with unbiased polymer translocation.

PACS numbers: 05.40.-a, 82.35.Lr, 87.15.A-, 87.15.H-

## I. INTRODUCTION

There has been an ongoing interest in recent years in the analysis of models of polymer dynamics. The origin of this interest is due to two main facts. Firstly, experiments allow nowadays to control polymers at nanoscales and to follow the behavior of single molecules, providing thus many insights on their dynamics [1–3]. This has motivated more theoretical research in the field. Secondly, many of these systems show an anomalous dynamics, a paradigmatic example being that of a polymer translocating through a nanopore [4]. Modeling anomalous dynamics has attracted quite some attention in the Statistical Physics community due to the ubiquity of this behavior in many physical systems as disordered media [5], conformational fluctuations of proteins [6], diffusion of molecules in cells [7] and polymers [8].

In the case of polymer translocation, the subdiffusive behavior is inferred from the scaling  $\tau \sim L^\alpha$  with  $\alpha > 2$ , which relates the translocation time  $\tau$  to the polymer length  $L$ . Although there have been a large number of publications [4, 9–11] there is no general agreement on the value of  $\alpha$  obtained from simulations. Also on the theoretical side different predictions for  $\alpha$  have been made [4, 12, 13].

Besides translocation, there are other polymer processes which are expected to show anomalous dynamics. We are interested here in the analysis of zipping dynamics, which is the process through which two “complementary” strands attached by one end bind/unbind from each other, as shown in Fig. 1. In our model we do not allow bubbles to be formed, hence the dynamics proceeds sequentially as in a zipper. We focus here on the dynamics at the transition temperature  $T = T_c$ . At low temperatures ( $T < T_c$ ) the system is driven towards the fully zipped state (Fig. 1(c)), whereas at high tempera-

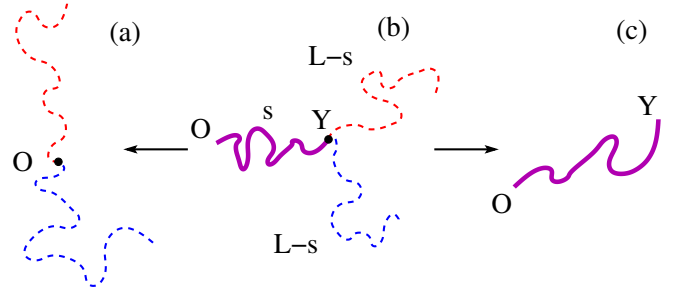


FIG. 1. (Color online) Sketch of the zipping/unzipping dynamics. The two polymer strands are joined by a common end O. Single stranded polymers are shown as dashed lines, while double stranded as a thick solid line. (a) Fully unzipped state, (b) Partially zipped, (c) Fully zipped. Y denotes the position of the end of the double stranded segment. The total length of each strand is  $L$ . A partially zipped configuration is characterized by two single strands of length  $L - s$  and a double strand of length  $s$ .

tures ( $T > T_c$ ) the two strands unbind (Fig. 1(a)). The dynamics for these two cases were studied in Ref. [14]. Interestingly, the zipping time was found to scale as the length of the polymer as  $\tau_z \sim L^\alpha$  with  $\alpha \approx 1.37$ , whereas the unzipping time scaled as  $\tau_u \sim L$ . If the dynamics were sufficiently slow (see below), so that zipping and unzipping proceed through quasi-equilibrium states, the times would scale linearly in the strand length  $L$ . This corresponds to the motion of a Brownian particle, the fork point Y shown in Fig. 1(b), in a linear downhill potential. A scaling  $\tau_z \sim L^\alpha$  with  $\alpha \neq 1$  implies anomalous dynamics. We note, in addition, that the anomalous exponent for zipping ( $\alpha = 1.37$ ) turns out to be in agreement with that found in some simulations of forced polymer translocation [15, 16].

We recall that in forced (or biased) translocation an

external field drives the polymer preferentially towards one of the two sides of the separating membrane. This can be realized experimentally, for instance for a charged polymer as DNA or RNA by imposing an electric potential difference on the two sides. In unbiased translocation the external field is absent and the polymer translocation is driven by thermal fluctuations.

The aim of this paper is to extend the analysis of the zipping dynamics to the critical temperature  $T = T_c$ . In this case there is no strong bias towards either the zipped or unzipped state, as these two have the same free energy in the thermodynamic limit. One could therefore expect an analogous behavior of that found in unbiased polymer translocation. However, the exponent we find in our simulations disagrees with those conjectured for unbiased translocation suggesting that critical zipping is in another universality class. We find however that the underlying stochastic process is well-described by a fractional Brownian motion [17] for which we determine the Hurst exponent, probability distribution function and survival probabilities.

## II. MODEL

The model discussed here was also used in recent studies of renaturation dynamics [18] and zipping dynamics [14]. Two polymers defined on a face-centered-cubic (fcc) lattice are joined by a common end. The monomers on both strands are labeled by an index  $i = 0, 1, \dots, L$ . The two strands are self- and mutually avoiding, with the exception of monomers with the same index  $i$ , which are referred to as complementary monomers. Two complementary monomers can bind by overlapping on the same lattice site. A typical simulation run start with all monomers  $0 \leq i \leq L/2$  bound, and the monomers  $i > L/2$  unbound (see Fig. 1(b)). This initial configuration is relaxed to equilibrium by means of pivot [19] and local moves which leave the number of bounded monomers unchanged. Once an equilibrium configuration is obtained the actual simulation is started. The pivot algorithm is no longer used and the Monte Carlo updates are strictly local. They consist of corner-flip or end-flip moves that do not violate self- and mutual avoidance. **A feature of the fcc lattice geometry is that the local moves are such that two different polymer chains cannot intersect each other. In the simple cubic geometry the non-crossing condition can be realized by the bond-fluctuation model [20]. The local dynamics on the fcc lattice reproduces the Rouse model behavior, as shown in [21].**

A Boltzmann weight  $\omega > 1$  is associated to the binding of two monomers. In the Monte Carlo dynamics binding occurs with probability 1 while unbinding with probability  $1/\omega$ , so that detailed balance is satisfied. A Monte Carlo step consists in selecting a random monomer on one of the two strands. If the selected monomer is unbound a

local flip move is attempted. If the selected monomer is a bound monomer there are two possibilities. Either a local flip of the chosen monomer is attempted, and if accepted, this move results in the bond breakage; or a flip move of both bound monomers is generated, which does not break the bond between them. In the model discussed here we do not allow any bubble formation neither for zipping nor unzipping, by imposing the constraint that monomer  $i$  can bind to its complement only if monomer  $i - 1$  is already bound. Analogously monomer  $i$  can unbind only if monomers  $i + 1$  are already unbound. This is the model Y which was referred to in Ref. [14]. As unit of time we take  $2L + 1$  Monte Carlo steps, so that in one time step one attempted update per monomer is performed.

## III. EQUILIBRIUM FREE ENERGIES

We start by discussing some properties of the equilibrium free energy of zipping polymers. We consider in particular the dependence of this free energy on the coordinate  $s$ , describing the position of a fictitious Brownian particle. We analyze the motion of this particle in the given free energy landscape.

The number of configurations for a linear polymer of length  $L$ , in the limit of  $L \rightarrow \infty$ , takes the asymptotic form  $Z \sim \mu^L L^{2\sigma_1}$  where  $\mu$  is the connectivity constant and  $\sigma_1$  a universal exponent associated to the end vertex of the polymer [22] (we use here a different notation from the customary exponent  $\gamma = 1 + 2\sigma_1$ ). In general the partition function of polymer networks of more complex topology [23] is also characterized by subleading universal exponents. For instance a star polymer with three arms of length  $L$  has a partition function scaling as  $Z_3 \sim \mu^{3L} L^{\sigma_3 + 3\sigma_1}$ , with  $\sigma_3$  the exponent associated to a vertex with three outgoing arms. Here the factor  $3\sigma_1$  accounts for the three end vertices.

We can now consider the case of partially zipped polymer strands of Fig. 1(b), which is related to that of a three arms star polymer. We allow now the three arms to have lengths  $L - s$  and  $s$ . In addition we have to account for the Boltzmann weight  $\omega$  associated to the binding between the  $s$  monomers on the double stranded segment. The total partition function is then given by

$$Z(s) = \mu^{2L-s} \omega^s L^{3\sigma_1 + \sigma_3} f(s/L) \quad (1)$$

where  $f(x)$  a scaling function. We analyze now the limiting scaling behavior of the partition function (1). For  $s \rightarrow 0$  one should recover the partition function of a single polymer of length  $2L$  which yields  $f(x) \sim x^{\sigma_1 + \sigma_3}$ . The analysis of the limit  $s \rightarrow L$  similarly imposes  $f(x) \sim (1 - x)^{\sigma_1 + \sigma_3}$ . One can incorporate the two limits in the following expression:

$$Z(s) = \mu^{2L-s} \omega^s L^{3\sigma_1 + \sigma_3} \left(\frac{s}{L}\right)^{\sigma_1 + \sigma_3} \left(1 - \frac{s}{L}\right)^{\sigma_1 + \sigma_3} g(s/L) \quad (2)$$

with  $g(x)$  an analytic function of its variable.

We distinguish now two cases:  $\omega \neq \mu$  and  $\omega = \mu$ , which correspond to the off-critical and to the critical case, respectively. If  $\omega \neq \mu$  the leading dependence on  $s$  of the free energy is

$$f(s) = -\log Z(s) \sim -s \log(\omega/\mu) \quad (3)$$

where the constant terms, and subleading terms in  $s$  have been omitted. For  $\omega > \mu$  the zipped state (low temperature phase) is favored, whereas  $\omega < \mu$  favors unzipping (high temperatures). Viewing  $s$  as a zipping coordinate one can consider a Fokker-Planck (FP) description of the process, which is the motion of a Brownian particle on a potential  $f(s)$ . For  $\omega \neq \mu$  the potential is linear in  $s$  (Eq. (3)), equivalent to a biased Brownian motion towards  $s = 0$  ( $\omega < \mu$ ) or  $s = L$  ( $\omega > \mu$ ). In both cases the characteristic time of the particle for starting in one boundary to reach the opposite one scales as  $\sim L$ .

At the critical point ( $\omega = \mu$ ) the free energy becomes

$$f(s) = -(\sigma_1 + \sigma_3) \log \left[ \frac{s}{L} \left( 1 - \frac{s}{L} \right) \right] - \log g(s/L) \quad (4)$$

(omitting terms which do not depend on  $s$ ). We compare now this expression with the free energy of translocating polymers. Consider a polymer on a pore of an infinitely wide separating plane. The pore divides the polymer into two non interacting parts of lengths  $s$  and  $L - s$  respectively. The two parts are characterized by partition functions  $Z_1 \sim \mu^s s^{\gamma_s - 1}$  and  $Z_2 \sim \mu^{L-s} (L - s)^{\gamma_s - 1}$ , where  $\gamma_s$  is an entropic exponent associated to a polymer attached to a planar surface. One obtains the equilibrium free energy of the polymer on the pore [4]:

$$f_t(s) = -(\gamma_s - 1) \log \left[ \frac{s}{L} \left( 1 - \frac{s}{L} \right) \right] \quad (5)$$

This free energy has a strong analogies with that of the zipping polymer at  $T_c$  (Eq. 4). One difference is the value of the exponent. For a three dimensional self-avoiding walk attached to a planar surface  $\gamma_s = 0.70$  [22], whereas from renormalization group results [24] one finds  $\sigma_1 + \sigma_3 \approx -0.08$ .

In an early study of translocation, Chuang et al. [4] analyzed the FP equation corresponding to a Brownian particle moving in the potential (5). Within this framework they showed that, by appropriate rescaling of polymer length  $L$ , time and space coordinates one finds a translocation time scaling as  $\tau_t^{FP} \sim L^2$ , independently on the value of  $\gamma_s$ . A similar rescaling is also applicable to the free energy in Eq. (4), even in the presence of an analytic scaling function  $g(x)$ . The analysis thus shows that the zipping/unzipping time  $\tau_{z/u}^{FP} \sim L^2$ . However it was also argued [4] that this result is not self-consistent as the time required for a polymer to equilibrate (the Rouse time,  $\tau_R \sim L^{1+2\nu}$  and  $\nu \approx 0.59$  in three dimensions thus  $\tau_R \sim L^{2.18}$ ) turns out to be longer than the predicted  $\sim L^2$  from the FP equation. In conclusion a polymer cannot translocate through quasi-equilibrium states, because it would do so at a rate at which it cannot equilibrate [4]. A similar reasoning can be applied

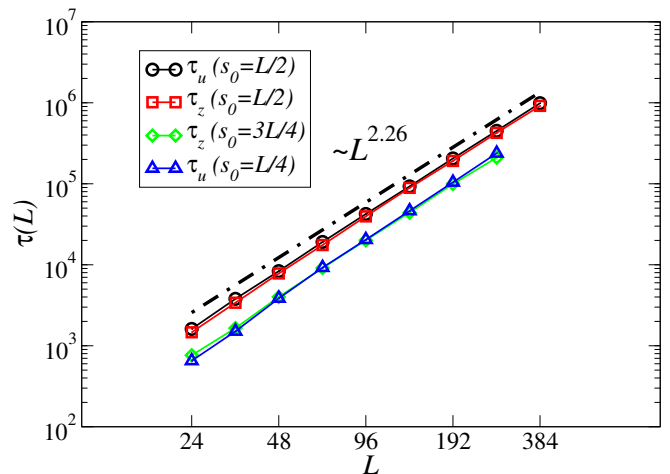


FIG. 2. (Color online) Log-log plot of the zipping ( $\tau_z$ ) and unzipping ( $\tau_u$ ) times as functions of the strand lengths  $L$ . The two quantities scale with the same anomalous exponent  $\tau_z \sim \tau_u \sim L^{2.26(2)}$ . Circles and squares are data from simulations with initial condition  $s_0 = L/2$ , i.e. half-zipped configurations. Diamonds correspond to the zipping time using as initial condition  $s_0 = 3L/4$ . Triangles correspond to the unzipping time with initial condition  $s_0 = L/4$ .

to the potential of zipping strands (Eq. (4)). It can be shown that the modulating scaling function  $g(x)$  does not alter the general result and thus the FP equation predicts a zipping time scaling as  $\tau \sim L^2$ . As for translocation, however, this result is not self-consistent since the equilibration time of the polymer would then exceed the zipping/unzipping time. One deduces also for zipping at  $T_c$  a lower bound  $\tau_{z/u} \geq L^{1+2\nu}$  of the zipping/unzipping time.

## IV. SIMULATION RESULTS

### A. Scaling of zipping/unzipping times

The simulations at  $T = T_c$  are started from a configuration with  $s = s_0$ , i.e. with a star polymer with a double stranded segment of length  $s_0$  and two single strands of length  $s - s_0$ . The critical point is obtained by setting the Boltzmann weight of binding of two monomers to  $\omega = \mu$ . The connectivity constant for self-avoiding polymers in a fcc lattice is known with a high degree of accuracy  $\mu = 10.0362(6)$  [25], which provides  $T_c$  with a very good precision. The initial configuration is thermalized while keeping  $s$  fixed. This constraint is released at time  $t = 0$  and the simulation is stopped once one of the two boundaries  $s = 0$  or  $s = L$  is reached. These boundaries correspond to fully unzipped strands and to fully zipped strands, respectively (see Fig. 1(a) and (c)). The simulations are repeated typically for  $10^4$  different realizations.

Figure 2 shows a plot of the averages of the zipping  $\tau_z$

and unzipping  $\tau_u$  times as a function of the strand length. Error bars are smaller than symbol sizes. The four different data sets correspond to different initial conditions  $s_0 = L/2$  (half-unzipped),  $s_0 = L/4$  and  $s_0 = 3L/4$ . Apart from small deviations, for very short polymers, the data show a power-law behavior which is described by the same exponent  $\tau_z \sim \tau_u \sim L^{2.26(2)}$ . Note that for  $s_0 = L/2$  the unzipping is systematically slightly slower than zipping ( $\tau_u > \tau_z$ ). The differences are due to the asymmetry of the problem with respect to the interchange  $s \rightarrow L - s$ . This asymmetry has seemingly not a strong effect on the dynamics; it only influences  $\tau_z$  and  $\tau_u$  by a multiplicative factor, but it does not change the exponent. The exponent  $\alpha = 2.26(2)$  indicates a subdiffusive behavior. In addition the expected lower bound  $\tau_R \sim L^{1+2\nu}$ , discussed above, is verified. But clearly  $\alpha > 1 + 2\nu = 2.18$ . Also notice that  $\alpha$  is considerably lower than the value  $2 + \nu = 2.58$  recently conjectured for unbiased translocation [12].

### B. Probability distribution function (pdf)

We computed next  $P(s, t)$ , the probability distribution function (pdf) of the value of  $s$  at time  $t$ . Initially, at time  $t = 0$ , one has  $P(s, 0) = \delta(s - s_0)$ , whereafter  $P(s, t)$  spreads in time. Here we consider the case  $s_0 = L/2$ . The shape of the distribution at later times gives some insights on the nature of the underlying stochastic process. It has been recently suggested [26, 27] that unbiased translocation could be described by a class of processes known as fractional Brownian motion (fBm). The fBm [17] is a Gaussian, self-affine process with stationary increments. It is described by a probability distribution with a Gaussian shape, but with variance growing as a power law in time, i.e.

$$P(s, t) = \frac{1}{\sqrt{2\pi Dt^{2H}}} \exp\left[-\frac{(s - s_0)^2}{4Dt^{2H}}\right] \quad (6)$$

where  $s_0 = L/2$  in our setup (the starting point of the simulations) and  $D$  is a constant. Here  $0 < H < 1$  is known as the Hurst exponent;  $H = 1/2$  corresponds to Brownian motion.  $H < 1/2$  and  $H > 1/2$  are the subdiffusive and the superdiffusive cases. The distribution (6) cannot hold at all times, due to the presence of boundaries at  $s = 0$  and  $s = L$ .

Figure 3 (main graph) shows plots of  $P(s, t)/P(L/2, t)$  vs.  $s$  on a log-linear scale at different times for strands of length  $L = 192$ , averaged over  $10^5$  histories. In these simulations,  $P(s, t)$  is calculated from the surviving samples, i.e. those which never reach the boundaries  $s = 0$  and  $s = L$  at time  $t$ . Similar results were obtained for other  $L$ -values. One observes the spreading of the distribution from its initial delta shape. For large times,  $P(s, t)$  converges to a stationary distribution whose properties we will discuss below.

As a check whether (and when) these data can be described by a Gaussian distribution we have calculated the

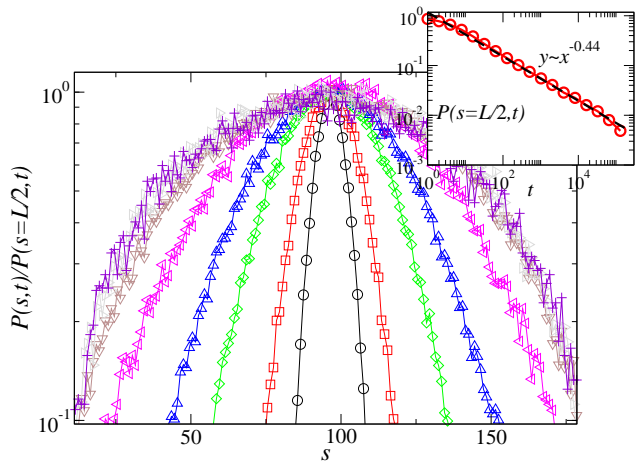


FIG. 3. (Color online) Plot of  $P(s, t)/P(L/2, t)$  for strands of length  $L = 192$  for different simulation times  $t = 2^9, 2^{11}, 2^{13}, 2^{14}, 2^{15}, 2^{16}, 2^{17}$  and  $2^{18}$ . The inset shows  $P(s = L/2, t)$  versus time in a log-log plot.

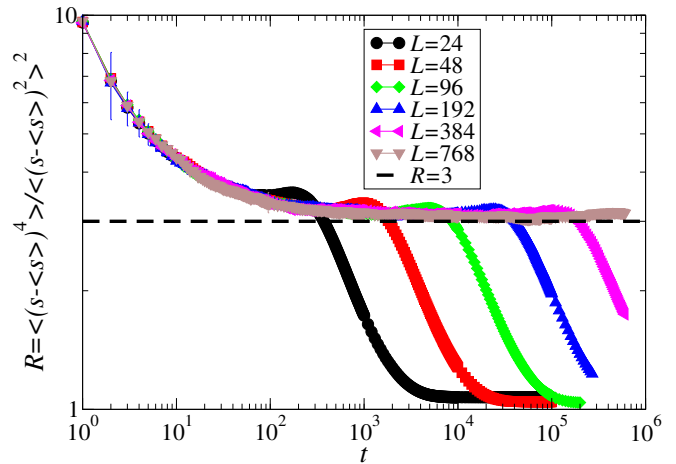


FIG. 4. (Color online) Plot of  $R = \langle (s - \langle s \rangle)^4 \rangle / \langle (s - \langle s \rangle)^2 \rangle^2$  as a function of time for various  $L$ -values. The dashed line indicates the Gaussian value  $R = 3$ . The sampling is over  $5 \cdot 10^5$  configurations for  $L = 24, 48$ ,  $2 \cdot 10^5$  configurations for  $L = 96$  and  $10^5$  configurations for  $L = 192, 384, 768$ .

ratio  $R \equiv \langle (s - \langle s \rangle)^4 \rangle / \langle (s - \langle s \rangle)^2 \rangle^2$  which for a Gaussian equals 3. Results for  $R$  as a function of time and for various values of  $L$  are shown in Figure 4. These data show that after an initial regime the gaussian value is **very slowly** approached. After a time of the order of the zipping/unzipping time, the boundaries are being felt, and a deviation from the Gaussian value develops, as should be expected. The extrapolation for different values of  $L$  yields  $R = 3.04(5)$ , consistent with a gaussian distribution.

We next turn to the determination of the exponent  $H$ . This can be done in two ways. Firstly, we looked at  $P(s = L/2, t)$  which should decay as  $t^{-H}$ . As can be

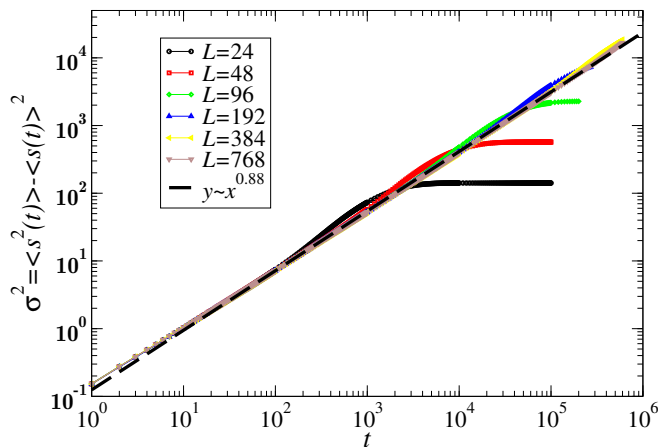


FIG. 5. (Color online) Plot of  $\sigma^2$  as a function of time  $t$  for different values of  $L$ . The dashed line is a power-law fit to the data, yielding  $H = 0.44$ .

seen in the inset of Fig. 3 our results are well fitted with a power law. From an analysis of the data for various  $L$ -values we arrive at the estimate  $H = 0.44(1)$ .

Secondly, we determined the scaling of the variance of the position distribution,  $\sigma^2(t) = \langle (s - \langle s \rangle)^2 \rangle$ , as a function of time. For the Gaussian distribution (6) one has  $\sigma^2(t) \sim t^{2H}$ . For times above  $\tau_{z/u}$  deviations from this behavior appear and asymptotically in time  $\sigma^2$  should saturate at a value  $\sim L^2$ . We therefore expect a scaling of the form

$$\sigma^2(t) \sim t^{2H} F(t/\tau) \quad (7)$$

where  $F(x)$  is a scaling function and  $\tau$  is  $\tau_z$  or  $\tau_u$ .

This is precisely the behavior that we observe in our simulations (Fig. 5). From the initial power law increase we arrive at the independent estimate of  $H = 0.44(1)$ . Since at  $t \approx \tau$ ,  $\sigma^2 \sim L^2$  we obtain  $\tau_z \sim \tau_u \sim L^\alpha$  where  $\alpha = 1/H$ . For  $H = 0.44(1)$ ,  $\alpha = 2.27(2)$ , fully consistent with our results on the behavior of the zipping/unzipping times shown in Fig. 2. In conclusion, we find clear numerical evidence that the dynamics of the zipping coordinate  $s$  is well described by the distribution (6) with an exponent  $H = 0.44(1)$  in the time regime where  $t < \tau_{z/u}$ .

### C. Velocity autocorrelation

Since fBm is a Gaussian process, it is fully characterized by its average and covariance matrix. The latter, which can also be interpreted as a position correlation function, has the form [17]

$$\langle s(t_1)s(t_2) \rangle = D(t_1^{2H} + t_2^{2H} - |t_1 - t_2|^{2H}) \quad (8)$$

where  $D$  is a constant. The autocorrelation of the velocity  $v = ds/dt$  can be obtained by differentiation with respect to  $t_1$  and  $t_2$  [28]

$$\langle v(t_1)v(t_2) \rangle = \frac{d^2 \langle s(t_1)s(t_2) \rangle}{dt_1 dt_2} = -D \frac{d^2 |t_1 - t_2|^{2H}}{dt_1 dt_2}$$

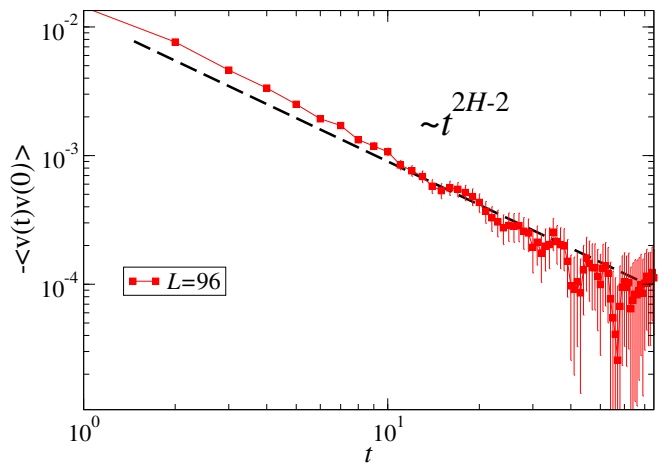


FIG. 6. (Color online) Log-log plot of minus the velocity autocorrelation as a function of time. The dashed line is a straight line (not a fit) with slope  $-1.12$ .

$$= 2H(2H - 1)D|t_1 - t_2|^{2H-2} + 2HD|t_1 - t_2|^{2H-1}\delta(t_1 - t_2)$$

Because of the stationarity of the process one obtains for  $t > 0$

$$\langle v(t)v(0) \rangle = 2H(2H - 1)Dt^{2H-2} \quad (9)$$

For a fBm with  $H < 1/2$  (subdiffusive), as is the case for zipping, this implies a negative velocity autocorrelation function. Using  $H = 0.44$  one finds  $2H - 2 = -1.12$ . In Fig. 6 we show our results for this quantity in a log-log plot. In order to compute  $\langle v(t)v(0) \rangle$  reliably more than  $10^7$  configurations were sampled, which is 100 more than typically done for other quantities. Still, the velocity autocorrelation could be estimated with sufficient precision only for short times ( $t < 10^2$ ). It is therefore difficult to obtain a good estimate of  $H$  from these data. The figure shows however that  $\langle v(t)v(0) \rangle$  is negative and decays with a power law as expected. The decay for  $t > 10$  is not inconsistent with the predicted value  $-1.12$ .

### D. Survival probability

Next, we look at the probability distribution of the (un)zipping time  $Q(\tau_{z/u}, L)$ . These results are plotted in Figure 7 for  $L = 24, 48, 96$  and  $192$  (only unzipping data are shown, the distributions for the zipping times are very similar). As seen from the figure, the probability distribution decays exponentially for long times. The data for different lengths collapse into a single scaling function (for  $L$  sufficiently large), where  $\tau/L^{2.26}$  is used as a scaling variable. The normalization condition of the probability distribution function implies the following scaling form:

$$Q(\tau, L) = L^{-2.26} f(\tau/L^{2.26}) \quad (10)$$

where  $f(x)$  is a scaling function which decays exponentially for large  $x$ . An exponential decay of the survival probability  $S(t)$ , which is related to the pdf of the (un)zipping time by  $Q(t) = -dS/dt$  is also characteristic for fBm with two absorbing boundaries [26]. These results also rule out a description of  $P(s, t)$  in terms of a fractional Fokker-Planck equation with absorbing boundaries for which  $Q(\tau)$  decays as a power law [29, 30].

### E. Boundary exponents

There has been quite some interest in the behavior of fractional Brownian motion in the vicinity of an absorbing boundary. For ordinary diffusion the probability distribution  $P(s, t)$  on the interval  $[0, L]$  becomes proportional to  $\sin(\pi s/L)$  asymptotically. This means that  $P(s, t)$  vanishes linearly with the distance  $y$  from an absorbing boundary. For a fBm with Hurst exponent  $H$  it has been recently argued [26] that the pdf vanishes as  $\sim y^\phi$ , with  $\phi = (1 - H)/H$ . For ordinary diffusion ( $H = 1/2$ ) this gives the correct result  $\phi = 1$ .

In view of this recent interest, we have investigated the behavior of the pdf near absorbing boundaries. In order to determine the boundary exponent  $\phi$  we have replotted in Figure 8 the results of Figure 3 in a log-log plot. According to Ref. [26] a fBm with a Hurst exponent  $H = 0.44$  would imply a boundary exponent  $\phi = 1.27$ . The corresponding power-law behavior is shown as a dashed line in Figure 8. This exponent is in good agreement with the numerical data at sufficiently long simulation times for which the distribution becomes stationary.

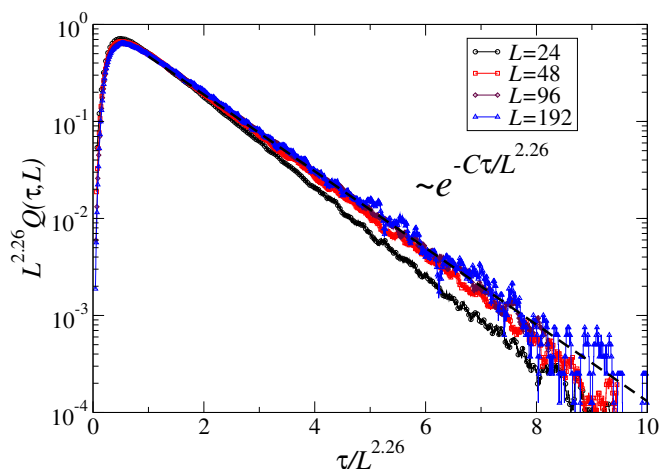


FIG. 7. (Color online) Linear-log plot of the scaling function of the probability distribution of the unzipping time for the sizes  $L = 24, 48, 96$  and  $192$ . The calculations are done over  $10^6$  configurations for  $L = 24, 48$  and  $96$  and over  $2 \cdot 10^5$  configurations for  $L = 192$ .

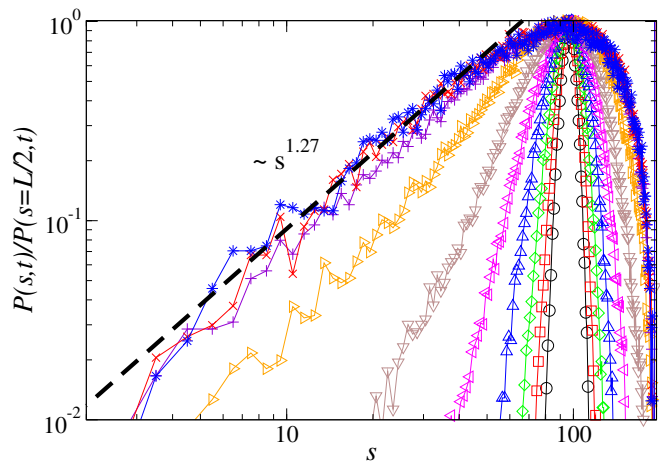


FIG. 8. (Color online) Plot of  $\ln P(s, t)$  vs.  $\ln s$  emphasizing the vanishing of the position pdf in the vicinity of the absorbing boundaries (same data as in Fig. 3,  $L = 192$  and times are  $t = 2^9, 2^{10}, \dots, 2^{17}, 2^{18}$ ). For the two longest simulation times the distribution is almost stationary and the probability distribution vanishes in agreement with a power-law behavior  $\sim s^{-1.27}$  (dashed line). This is the expected behavior for a fractional Brownian motion with  $H = 0.44$  in the vicinity of a boundary, as derived in Ref. [26].

## V. CONCLUSIONS

In this paper we have analyzed the dynamics of zipping polymers at their critical point by means of simulations of polymers undergoing Rouse dynamics. The natural coordinate describing the process is  $s$ , denoting the length of the double stranded (zipped) part of the strands. At  $T = T_c$  the equilibrium free energy has a form very similar to that of a polymer translocating through a membrane, i.e. a logarithmic dependence on  $s$ , except for a weakly modulating function, which is shown to have a weak effect on the dynamics.

Using the same arguments as for translocation one can derive a lower bound  $\tau_{z/u} \sim L^\alpha$  with  $\alpha \geq 1 + 2\nu \approx 2.18$ . The numerical results are indeed in agreement with this behavior, and provide an estimate  $\alpha \approx 2.26(2)$  which is higher than the lower bound value. Different exponents have been reported in the literature for polymer translocation (ranging from 2.23 [31], 2.51[32] to 2.59 [12]), but it should be noticed that critical zipping does not seem to share a common universal dynamical scaling behavior with unforced polymer translocation. This could be a bit surprising at first, as a recent study of zipping dynamics at  $T < T_c$  showed instead a good agreement with that found in forced polymer translocation [14]. On the other hand it also reported that that the unzipping dynamics at  $T > T_c$  is not anomalous ( $\tau_u \sim L$ ). At  $T = T_c$  the dynamics is a complex combination of zipping and unzipping resulting in an exponent that deviates from that for unbiased translocation.

It has been recently suggested that translocation could be described by fractional Brownian motion [26, 27, 33].

We have therefore considered the possibility that a fBm approach could also provide a consistent description of the critical zipping/unzipping dynamics. Our results show that this is indeed the case. On time scales smaller than the zipping/unzipping time, the distribution of the zipping coordinate  $s$  is well described by a Gaussian with a variance that grows as  $t^{2H}$  with  $H = 0.44(1)$ . In the presence of absorbing boundary conditions we find that  $P(s, t)$  conditioned on not being absorbed yet, converges to a distribution that behaves as a power law near the boundaries. The associated exponent  $\phi$  agrees with that recently determined for fBm [26].

Fractional Brownian motion has been observed in other

polymer processes, most notably in the fluctuations of the distance between an electron transfer donor and acceptor pair in single molecule experiments on proteins [6]. Recently, it has been argued that this complicated dynamics can arise from a superposition of Markovian fluctuations of normal modes as for example those present in the Rouse model [34]. It would be interesting to get further insight in the underlying dynamics of the zipping coordinate  $s$  in a similar spirit.

**Acknowledgement** We would like to thank G. Barkema, R. Metzler, D. Panja and A. Rosso for interesting discussions on the subject of this paper.

- 
- [1] D. Lumma, S. Keller, T. Vilgis, and J. O. Rädler, Phys. Rev. Lett. **90**, 218301 (2003)
  - [2] R. Shusterman, S. Alon, T. Gavrinov, and O. Krichevsky, Phys. Rev. Lett. **92**, 048303 (2004)
  - [3] E. P. Petrov, T. Ohrt, R. G. Winkler, and P. Schuille, Phys. Rev. Lett. **97**, 258101 (2006)
  - [4] J. Chuang, Y. Kantor, and M. Kardar, Phys. Rev. E **65**, 011802 (2001).
  - [5] J.-P. Bouchaud and A. Georges, Physics Reports **195**, 127 (1990).
  - [6] S. C. Kou and X. S. Xie, Phys. Rev. Lett. **93**, 180603 (2004)
  - [7] J.-H. Jeon, V. Tejedor, S. Burov, E. Barkai, C. Selhuber-Unkel, K. Berg-Sørensen, L. Oddershede, and R. Metzler, Phys. Rev. Lett. **106**, 048103 (2011)
  - [8] D. Panja, J. Stat. Mech.: Theory and Exp. **2010**, P06011 (2010).
  - [9] W. Sung and P. J. Park, Phys. Rev. Lett. **77**, 783 (1996)
  - [10] M. Muthukumar, J. Chem. Phys. **111**, 10371 (1999)
  - [11] J. K. Wolterink, G. T. Barkema, and D. Panja, Phys. Rev. Lett. **96**, 208301 (2006).
  - [12] D. Panja, G. T. Barkema, and R. C. Ball, J. Phys.: Condens. Matter **19**, 432202 (2007).
  - [13] T. Sakaue, Phys. Rev. E **81**, 041808 (2010).
  - [14] A. Ferrantini and E. Carlon, J. Stat. Mech.: Theory and Exp. **2011**, P02020 (2011).
  - [15] H. Vocks, D. Panja, G. T. Barkema, and R. C. Ball, J. Phys.: Condens. Matter **20**, 095224 (2008).
  - [16] K. Luo, T. Ala-Nissila, S.-C. Ying, and R. Metzler, Europhys. Lett. **88**, 68006 (2009).
  - [17] B. B. Mandelbrot and J. W. V. Ness, SIAM Review **10**, 422 (1968).
  - [18] A. Ferrantini, M. Baiesi, and E. Carlon, J. Stat. Mech.: Theory and Exp. **2010**, P03017 (2010).
  - [19] N. Madras and A. D. Sokal, J. Stat. Phys. **50**, 109 (1988).
  - [20] I. Carmesin and K. Kremer, Macromolecules **21**, 2819 (1988).
  - [21] A. Ferrantini, *Models of polymer dynamics: DNA renaturation and zipping* (PhD Thesis, KULeuven, 2011)
  - [22] C. Vanderzande, *Lattice Models of Polymers* (Cambridge University Press, Cambridge, 1998)
  - [23] B. Duplantier, Phys. Rev. Lett. **57**, 941 (1986)
  - [24] L. Schäfer, C. von Ferber, U. Lehr, and B. Duplantier, Nuclear Physics B **374**, 473 (1992).
  - [25] T. Ishinabe, Phys. Rev. B **39**, 9486 (1989)
  - [26] A. Zoia, A. Rosso, and S. N. Majumdar, Phys. Rev. Lett. **102**, 120602 (2009)
  - [27] J. L. A. Dubbeldam, V. G. Rostiashvili, A. Milchev, and T. A. Vilgis, Phys. Rev. E **83**, 011802 (2011)
  - [28] H. Qian, in *Processes with Long-Range Correlations: Theory and Applications*, Lecture Notes in Physics, Vol. 621, edited by G. Rangarajan and M.Z. Ding (Springer, New York, 2003), p. 22.
  - [29] S. B. Yuste and K. Lindenberg, Phys. Rev. E **69**, 033101 (2004)
  - [30] M. Gitterman, Phys. Rev. E **69**, 033102 (2004)
  - [31] D. Wei, W. Yang, X. Jin, and Q. Liao, J. Chem. Phys. **126**, 204901 (2007)
  - [32] C. Chatelain, Y. Kantor, and M. Kardar, Phys. Rev. E **78**, 021129 (2008)
  - [33] D. Panja, J. Phys. : Condens. Matter **23**, 105103 (2011)
  - [34] A. Dua and R. Adhikari, J. Stat. Mech. : Theory and Exp., P04017 (2011).